Double Synchronous Reference Frame PLL for Power Converters Control

P. Rodríguez(*), J. Pou(*), J. Bergas(*), I. Candela(*), R. Burgos(**) and D. Boroyevich(**)

(*)Technical University of Catalonia
(UPC)
Departments of Electrical and Electronic Engineering
Power Quality and Renewable Energy (QuPER)
EUETIT, Colom 1, 08222 – Terrassa - SPAIN
Email: prodriguez@ee.upc.edu

(**)Virginia Polytechnic Institute and State University
(Virginia Tech)
Department of Electrical and Computer Engineering
Center for Power Electronics Systems (CPES)
Blacksburg, VA 24061 - USA
Email: dushan@vt.edu

Abstract— This paper deals with one of the most important issues in the control of grid-connected converters, which is the detection of the positive sequence fundamental component of the utility voltage. The study carried out in this paper conducts to a fast, precise, and robust positive sequence voltage detector offering a good behavior, even if unbalanced and distorted conditions are present in the grid. The proposed detector utilizes a new "Double Synchronous Reference Frame PLL" (DSRF-PLL), which completely eliminates the existing errors in conventional synchronous reference frame PLL systems (SRF-PLL) when operating under unbalanced utility voltages.

In the study performed in this paper, the positive and negative sequence components of the unbalanced voltage vector are properly characterized. When this unbalanced vector is expressed on the DSRF, the analysis of the signals on the DSRF axes permits to design a decoupling network which isolates the positive and negative sequence components. This decoupling network gives rise to a new PLL structure which detects the positive sequence voltage component quickly and accurately. In this paper, conclusions of the analytical study are verified by simulation and experiment.

I. INTRODUCTION

One of the most important aspects to take into account in the control of power electronics working as power processor in power systems is the proper characterization of the utility voltage. In this field, detection of the positive sequence voltage component is essential in the control of power line conditioners, static VAR compensators, FACTS, UPS's and distributed generation systems [1][2]. Information about the positive sequence voltage is used for the synchronization of the converter output variables, power flux calculations or variable transformations to rotating reference frames. Regardless of the technique used in the system detection, the amplitude and the phase of the positive sequence component must be obtained quickly and accurately, even if the utility voltage is distorted and unbalanced.

There are two main approaches in the design of the positive sequence voltage detection algorithm. The first one assumes that the utility frequency is a constant and well-known magnitude. Under this assumption, the instantaneous symmetrical components method [3], or the algorithm based on the recursive weighted least-square estimation method [4], can be used. The second approach assumes that the utility frequency is not a constant parameter, and some algorithms based on different phase-locked loop (PLL) structures are used for the detection of the positive sequence component [5]-[7]. Commonly, these PLL structures are based on the "synchronous reference frame PLL" (SRF-PLL) technique [8][9].

As Fig. 1 shows, in the SRF-PLL the three-phase voltage vector is translated from the *abc* natural reference frame to the *dq* rotating reference frame by using the *Park* transformation [T_{dq}]. The angular position of this *dq* reference frame is controlled by a feedback loop which makes the *q* component equal to zero. Therefore, in steady-state, the *d* component will depict the voltage vector amplitude and its phase will be determined by the output of the feedback loop.

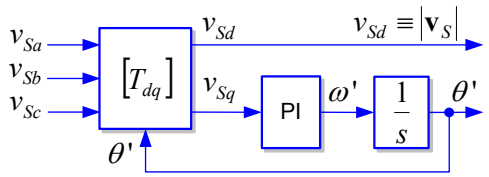

Fig. 1: Basic block diagram of the SRF-PLL.

Under ideal utility conditions, with neither imbalances nor harmonics, the SRF-PLL yields to good results. When high-order harmonic voltages appear, the PLL bandwidth can be reduced to reach a negligible effect of this harmonic on the output. But under voltage unbalancing, bandwidth reduction is not an acceptable solution, since the dynamic behavior of the PLL system becomes very poor [10], and the PLL output really deteriorated.

Therefore, in those situations in which unbalanced voltages are present in the utility and good dynamic behavior is required, the conventional SFR-PLL technique is not the most appropriate solution for the control of power converters.

0-7803-9033-4/05/$20.00 ©2005 IEEE.

In this work, the unbalanced voltage vector, consisting of positive and negative sequence components, is expressed on a "double synchronous reference frame" (DSRF). The study of the relationships between the signals on the different axes of this DSRF, and the designing of the proper decoupling system, gives rise to a new technique that can accurately obtain the phase and amplitude of the positive sequence utility voltage, even under unbalanced utility conditions. This new detection system has been named as "Double Synchronous Reference Frame PLL" (DSRF-PLL).

II. THE UNBALANCED VOLTAGE VECTOR ON THE DSRF

Under unbalanced utility conditions (without voltage harmonics), the voltage of the phase $i \in \{a,b,c\}$ can be generically expressed as:

$$v_{Si} = V_S^{+1}\cos\left(\omega t - k\tfrac{2\pi}{3}\right) + V_S^{-1}\cos\left(-\omega t - k\tfrac{2\pi}{3} + \phi^{-1}\right) + V_S^{0}\cos(\omega t + \phi^{0}), \quad (1)$$

where the superscript +1, -1 and 0 define coefficients of the positive, negative and zero sequence components, and $k = 0, 1, 2$ for $i = a, b, c$, respectively.

Using the non-normalized *Clarke* transformation, the utility voltage vector is given by:

$$\mathbf{v}_{S\,(\alpha\beta\gamma)} = \begin{bmatrix} v_{S\alpha} \\ v_{S\beta} \\ v_{S\gamma} \end{bmatrix}^{T} = \left[T_{\alpha\beta\gamma}\right]\begin{bmatrix} v_{Sa} \\ v_{Sb} \\ v_{Sc} \end{bmatrix}, \quad (2a)$$

$$\left[T_{\alpha\beta\gamma}\right] = \frac{2}{3}\begin{bmatrix} 1 & -\frac{1}{2} & -\frac{1}{2} \\ 0 & \frac{\sqrt{3}}{2} & -\frac{\sqrt{3}}{2} \\ \frac{1}{2} & \frac{1}{2} & \frac{1}{2} \end{bmatrix}. \quad (2b)$$

Neglecting the zero-sequence component, the expression of the voltage vector on the $\alpha\beta$ plane is:

$$\mathbf{v}_{S\,(\alpha\beta)} = \begin{bmatrix} v_{S\alpha} \\ v_{S\beta} \end{bmatrix} = \mathbf{v}_{S\,(\alpha\beta)}^{+1} + \mathbf{v}_{S\,(\alpha\beta)}^{-1} = V_S^{+1}\begin{bmatrix} \cos(\omega t) \\ \sin(\omega t) \end{bmatrix} + V_S^{-1}\begin{bmatrix} \cos(-\omega t + \phi^{-1}) \\ \sin(-\omega t + \phi^{-1}) \end{bmatrix}, \quad (3)$$

where it is evidenced that $\mathbf{v}_S$ consists of two subvectors: $\mathbf{v}_S^{+1}$, rotating with a positive angular frequency ω, and $\mathbf{v}_S^{-1}$, rotating with a negative angular frequency -ω.

A novelty in this paper is the fact of using a "double synchronous reference frame" (DSRF) which is composed of two rotating reference axes: dq^{+1}, rotating with the positive direction and whose angular position is θ', and dq^{-1}, rotating with the negative direction and whose angular position is $-\theta'$.

When the voltage vector $\mathbf{v}_S$ is expressed on a DSRF, equations (4) are obtained. In Fig. 2 these voltage vectors and reference frames are shown.

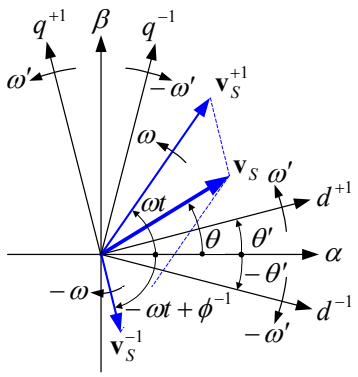

Fig. 2: Voltage vectors and axes of the DSRF.

$$\mathbf{v}_{S\,(dq^{+1})} = \begin{bmatrix} v_{Sd^{+1}} \\ v_{Sq^{+1}} \end{bmatrix} = \left[T_{dq^{+1}}\right]\cdot\mathbf{v}_{S\,(\alpha\beta)} = V_S^{+1}\begin{bmatrix} \cos(\omega t - \theta') \\ \sin(\omega t - \theta') \end{bmatrix} + V_S^{-1}\begin{bmatrix} \cos(-\omega t + \phi^{-1} - \theta') \\ \sin(-\omega t + \phi^{-1} - \theta') \end{bmatrix} \quad (4a)$$

$$\mathbf{v}_{S\,(dq^{-1})} = \begin{bmatrix} v_{Sd^{-1}} \\ v_{Sq^{-1}} \end{bmatrix} = \left[T_{dq^{-1}}\right]\cdot\mathbf{v}_{S\,(\alpha\beta)} = V_S^{+1}\begin{bmatrix} \cos(\omega t + \theta') \\ \sin(\omega t + \theta') \end{bmatrix} + V_S^{-1}\begin{bmatrix} \cos(-\omega t + \phi^{-1} + \theta') \\ \sin(-\omega t + \phi^{-1} + \theta') \end{bmatrix} \quad (4b)$$

$$\left[T_{dq^{+1}}\right] = \left[T_{dq^{-1}}\right] = \begin{bmatrix} \cos(\theta') & \sin(\theta') \\ -\sin(\theta') & \cos(\theta') \end{bmatrix} \quad (5)$$

Using a PLL structure, similar to that one showed in Fig. 1, and adjusting properly its control parameters, it is possible to achieve $\theta' \approx \omega t$. The election of this PLL control parameters is based on a small signal analysis in which is assumed $\sin(\omega t - \theta') \approx (\omega t - \theta')$, $\cos(\omega t - \theta') \approx 1$ and $(-\omega t - \theta') \approx -2\omega t$. In such conditions, (4) can be written as:

$$\mathbf{v}_{S\,(dq^{+1})} \approx V_S^{+1}\begin{bmatrix} 1 \\ \omega t - \theta' \end{bmatrix} + V_S^{-1}\begin{bmatrix} \cos(-2\omega t + \phi^{-1}) \\ \sin(-2\omega t + \phi^{-1}) \end{bmatrix}, \quad (6a)$$

$$\mathbf{v}_{S\,(dq^{-1})} \approx V_S^{+1}\begin{bmatrix} \cos(2\omega t) \\ \sin(2\omega t) \end{bmatrix} + V_S^{-1}\begin{bmatrix} \cos(\phi^{-1}) \\ \sin(\phi^{-1}) \end{bmatrix}. \quad (6b)$$

In (6), the constant values in the dq^{+1} and the dq^{-1} axes correspond to the amplitude of $\mathbf{v}_S^{+1}$ and $\mathbf{v}_S^{-1}$ respectively, and oscillations with 2ω frequency appear as a consequence of the coupling between axes and vectors with opposite rotation direction. This low-frequency oscillation could be attenuated by means of a low-pass filter, but the dynamic response of the detection system would be too slow. In order to cancel these oscillations, a decoupling network (DN) is presented in the following section. This DN obtains accurate results about the amplitude of $\mathbf{v}_S^{+1}$ and $\mathbf{v}_S^{-1}$, and the dynamic response of the detection system is improved.

III. DECOUPLING SIGNALS IN THE DSRF

To introduce the DN, one supposes a voltage vector consisting of two generic components rotating with $n\omega$ and $m\omega$ frequencies respectively, where m and n can be either positive or negative. This voltage vector is shown in (7).

$$\begin{aligned}\mathbf{v}_{S\,(\alpha\beta)} &= \begin{bmatrix} v_{S\alpha} \\ v_{S\beta} \end{bmatrix} = \mathbf{v}^{n}_{S\,(\alpha\beta)} + \mathbf{v}^{m}_{S\,(\alpha\beta)} \\ &= V_S^n \begin{bmatrix} \cos(n\omega t + \phi^n) \\ \sin(n\omega t + \phi^n) \end{bmatrix} + V_S^m \begin{bmatrix} \cos(m\omega t + \phi^m) \\ \sin(m\omega t + \phi^m) \end{bmatrix}\end{aligned} \tag{7}$$

Moreover, we are going to consider two rotating reference frames, dq^n and dq^m, whose angular positions are $n\theta'$ and $m\theta'$, respectively, being θ' the phase angle detected by the PLL. Finally, it is assumed $\theta' = \omega t$, where ω is the fundamental utility frequency. Therefore, the voltage vector can be expressed on these reference frames as follows:

$$\begin{aligned}\mathbf{v}_{S\,(dq^n)} &= \begin{bmatrix} v_{Sd^n} \\ v_{Sq^n} \end{bmatrix} = V_S^n \begin{bmatrix} \cos(\phi^n) \\ \sin(\phi^n) \end{bmatrix} \\ &+ V_S^m \cos(\phi^m) \begin{bmatrix} \cos((n-m)\omega t) \\ -\sin((n-m)\omega t) \end{bmatrix} \\ &+ V_S^m \sin(\phi^m) \begin{bmatrix} \sin((n-m)\omega t) \\ \cos((n-m)\omega t) \end{bmatrix},\end{aligned} \tag{8a}$$

$$\begin{aligned}\mathbf{v}_{S\,(dq^m)} &= \begin{bmatrix} v_{Sd^m} \\ v_{Sq^m} \end{bmatrix} = V_S^m \begin{bmatrix} \cos(\phi^m) \\ \sin(\phi^m) \end{bmatrix} \\ &+ V_S^n \cos(\phi^n) \begin{bmatrix} \cos((n-m)\omega t) \\ \sin((n-m)\omega t) \end{bmatrix} \\ &+ V_S^n \sin(\phi^n) \begin{bmatrix} -\sin((n-m)\omega t) \\ \cos((n-m)\omega t) \end{bmatrix}.\end{aligned} \tag{8b}$$

In (8), the amplitude of the signal oscillation in the dq^n axes depends on the mean value of the signal in the dq^m axes, and vice versa. In order to cancel the oscillations in the dq^n axes signals, the decoupling cell (DC) shown in Fig. 3(a) is proposed. For canceling the oscillations in the dq^m axes signals, the same structure of the DC can be used but swapping m and n superscripts in the variables.

Logically, for a correct operation of both DCs it is necessary to design some mechanism to determine the value of $\bar{v}^n_{Sd}$, $\bar{v}^n_{Sq}$, $\bar{v}^m_{Sd}$ and $\bar{v}^m_{Sq}$. Keeping this goal in mind, the decoupling network (DN) shown in Fig. 3(b) is proposed. In this DN, the LPF block is a low-pass filter such as:

$$LPF(s) = \frac{\omega_f}{s + \omega_f} \tag{9}$$

The following signals are defined for analyzing the DN:

$$u_1 = \cos((n-m)\omega t) \;\; ; \;\; u_2 = \sin((n-m)\omega t)\,. \tag{10}$$

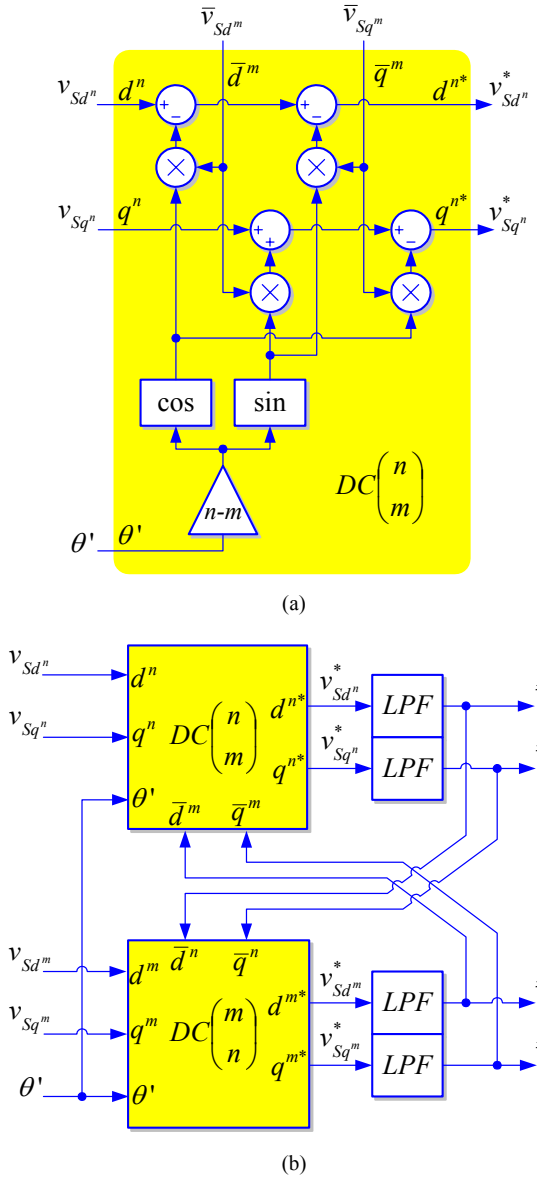

Fig. 3: (a) Decoupling cell for canceling the effect of $\mathbf{v}^m_S$ on the dq^n frame signals, (b) Decoupling network of dq^n and dq^m reference frames.

Using the variables of (10), the proper analytical development gives rise to the following expressions:

$$\dot{\bar{v}}_{Sd^n} = \omega_f \left(v_{Sd^n} - \bar{v}_{Sd^n} - u_1 \bar{v}_{Sd^m} - u_2 \bar{v}_{Sq^m} \right), \tag{11a}$$

$$\dot{\bar{v}}_{Sq^n} = \omega_f \left(v_{Sq^n} - \bar{v}_{Sq^n} - u_1 \bar{v}_{Sq^m} + u_2 \bar{v}_{Sd^m} \right), \tag{11b}$$

$$\dot{\bar{v}}_{Sd^m} = \omega_f \left(v_{Sd^m} - \bar{v}_{Sd^m} - u_1 \bar{v}_{Sd^n} + u_2 \bar{v}_{Sq^n} \right), \tag{11c}$$

$$\dot{\bar{v}}_{Sq^m} = \omega_f \left(v_{Sq^m} - \bar{v}_{Sq^m} - u_1 \bar{v}_{Sq^n} - u_2 \bar{v}_{Sd^n} \right). \tag{11d}$$

Finally, from (8), (10) and (11), the state-space model shown in (12) can be written.

$$\dot{\mathbf{x}}(t) = \mathbf{A}(t)\cdot\mathbf{x}(t) + \mathbf{B}(t)\cdot\mathbf{v}(t) \quad ; \quad \mathbf{y}(t) = \mathbf{C}\cdot\mathbf{x}(t), \tag{12a}$$

where:

$$\mathbf{x}(t) = \mathbf{y}(t) = \begin{bmatrix} \bar{v}_{Sd^n} \\ \bar{v}_{Sq^n} \\ \bar{v}_{Sd^m} \\ \bar{v}_{Sq^m} \end{bmatrix} \quad ; \quad \mathbf{v}(t) = \begin{bmatrix} V_S^n \cos(\phi^n) \\ V_S^n \sin(\phi^n) \\ V_S^m \cos(\phi^m) \\ V_S^m \sin(\phi^m) \end{bmatrix} \quad ; \quad \mathbf{A}(t) = -\mathbf{B}(t) \quad ; \quad \mathbf{C} = \mathbf{I}\,; \tag{12b}$$

$$\mathbf{B}(t) = \omega_f \begin{bmatrix} 1 & 0 & \cos((n-m)\omega t) & \sin((n-m)\omega t) \\ 0 & 1 & -\sin((n-m)\omega t) & \cos((n-m)\omega t) \\ \cos((n-m)\omega t) & -\sin((n-m)\omega t) & 1 & 0 \\ \sin((n-m)\omega t) & \cos((n-m)\omega t) & 0 & 1 \end{bmatrix}. \tag{12c}$$

State-space model of (12) corresponds to a multiple-input-multiple-output linear time variant system. Since the analytic solution of this system is really complex, its response will be evaluated considering $n = +1$ and $m = -1$, that is, decoupling the positive and negative fundamental frequency components in the dq^{+1} and dq^{-1} axes. Moreover, in order to simplify even more the solving process, it will be considered that $\phi^{+1} = 0$ and $\phi^{-1} = 0$. When $\mathbf{v}(t)$ is suddenly applied, like a step, expression (13) is obtained, which corresponds to the amplitude estimation of $\mathbf{v}_S^{+1}$.

$$\bar{v}_{Sd^{+1}} = V_S^{+1} - \left\{ V_S^{+1}\cos(\omega t)\cos\left(\omega t\sqrt{1-k^2}\right) \right. \tag{13}$$

$$\left. - \frac{1}{\sqrt{1-k^2}}\left(V_S^{+1}\sin(\omega t) - kV_S^{-1}\cos(\omega t)\right)\sin\left(\omega t\sqrt{1-k^2}\right)\right\} e^{-k\omega t}$$

In (13), the coefficient k is the rate between the cut-off frequency of the LPF and the fundamental utility frequency ($k = \omega_f / \omega$). In Fig. 4, expression (13) is plotted for different values of k (the rest of the variables get a set of fixed values according to the caption of Fig. 4). Oscillatory terms in (13) are affected by an exponential decay, therefore after a stabilization period defined by k, the amplitude of $\mathbf{v}_S^{+1}$ will be perfectly determined. If k>1 the dynamic response is underdamped.

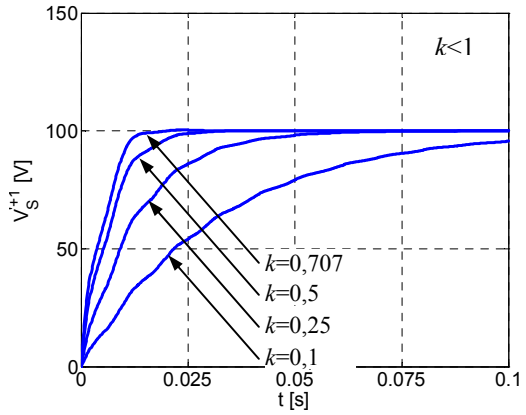

Fig. 4: Theoretical evolution of $\bar{v}_{Sd^{+1}}$ for different values of k, being $V_S^{+1} = 100\text{V}$, $V_S^{-1} = 30\text{V}$ and $\omega = 2\pi 50\text{rad/s}$

From the plots shown in Fig. 4, it seems logical to establish $k = 1/\sqrt{2}$, since the dynamic response is fast enough and does not appear oscillations in the amplitude estimation of $\mathbf{v}_S^{+1}$. It is worth to say that (13) comes from a small signal analysis, where it is assumed $\theta' \approx \omega t$. Taking into account that θ' is obtained by means of the PLL in the real system, certain transitory errors may appear in the dynamic response in relation to the theoretical response shown in Fig. 4, until PLL is not perfectly synchronized.

The higher value assigned to k, the faster response. Nevertheless it is necessary to note that transitory error in the system response will be also higher, which can give rise to an unstable behavior of the detection system. This justifies why the value of k should not be too high in order to reduce oscillations in the response and make the detection system more stable. This constrain in the maximum value of k is even more important when the utility voltages not only presents imbalance at the fundamental frequency but also high order harmonics.

IV. STRUCTURE AND BEHAVIOR OF THE DSRF-PLL

The block diagram of the DSRF-PLL proposed in this paper is shown in Fig. 5. In this diagram a conventional three-phase SRF-PLL structure is being used [9], but its behavior is improved by means of the DN.

In a conventional SRF-PLL, the objective of the PLL control loop is to achieve $v_{Sq^{+1}} = 0$. Under unbalanced utility voltage conditions, the control loop bandwidth of this conventional system must be strictly reduced in order to permit oscillations with 2ω frequency in $v_{Sq^{+1}}$. Bandwidth reduction can achieve the mean value of v_{Sd} to be close to the amplitude of the positive sequence voltage component. Using a high-order low-pass filter, the mean value of v_{Sd} can be obtained to estimate the amplitude of the positive sequence voltage component. This technique has two limitations: *i)* the true amplitude of the positive sequence component is not detected, but only an approximation, and *ii)* the dynamic response of the system is very poor.

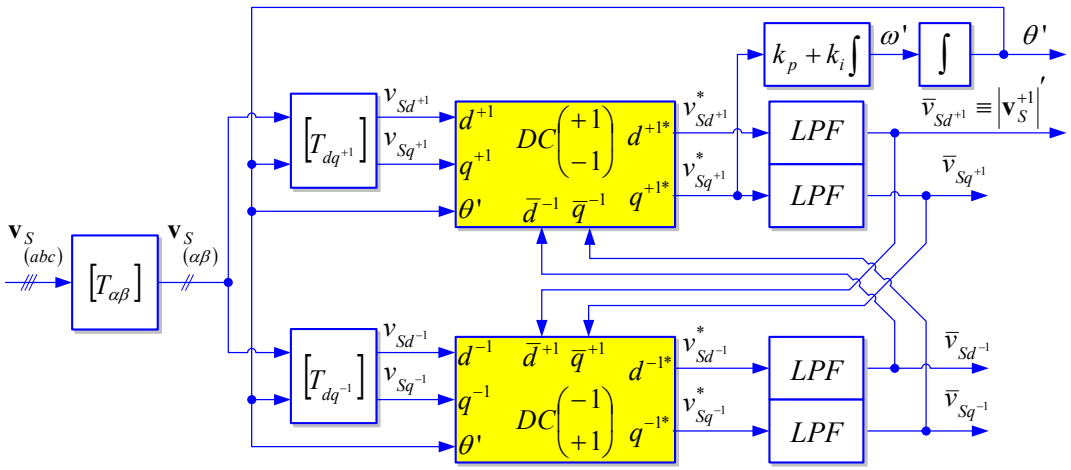

Fig. 5: Block diagram of the DSRF-PLL

When the DN is used in the DSRF-PLL, the oscillations at 2ω frequency are canceled in $v^*_{Sq^{+1}}$. Therefore, the control loop bandwidth can be increased in relation to the previous case, and the amplitude of the positive sequence voltage component will be detected accurately.

To show the good behavior of the proposed SDRF-PLL, similar grid conditions to those used to obtain Fig. 4 are considered in the simulation, that is, the unbalanced utility voltage is characterized by $V_S^{+1} = 100\text{V}$, $V_S^{-1} = 30\text{V}$, $\phi^{+1} = \phi^{-1} = 0$ rad, and $\omega = 2\pi 50$ rad/s. Fig. 6(a) shows this unbalanced utility voltage. Moreover, the tuning parameters for the DSRF-PLL are $k = 1/\sqrt{2}$, $k_p = 2{,}22$ and $k_i = 246{,}7$. The selection of k_p and k_i is based on a small-signal analysis which is reported in [6].

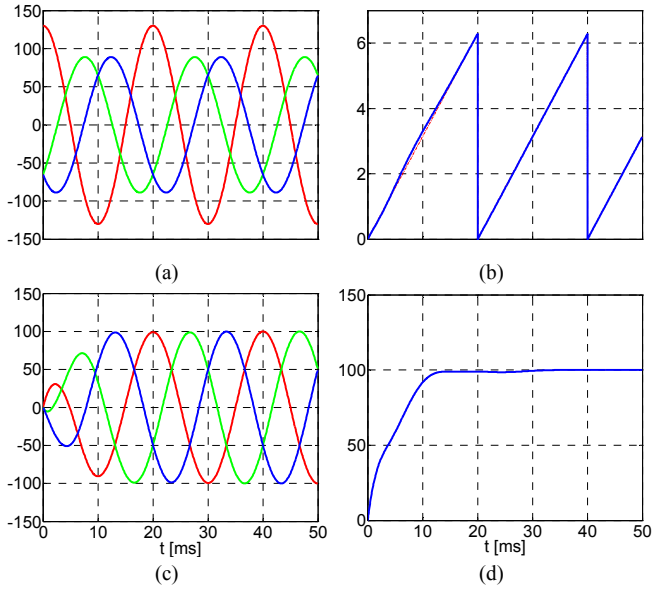

Fig. 6: Simulation results: (a) Utility voltage, $\mathbf{v}_S$ [V], (b) Detected phase angle, θ' [rad], (c) Detected positive sequence voltages, $\mathbf{v}_S^{+1}{}'$ [V], (d) Detected amplitude, $|\mathbf{v}_S^{+1}|'$ [V].

Fig. 6(b) and 6(d) show the detected phase angle and the amplitude for the positive sequence voltage component, respectively. From this information, the positive sequence voltage can be easily reconstructed, and the waveforms shown in Fig. 6(c) are finally obtained. In Fig. 6(c) it is possible to notice how the positive sequence component is perfectly obtained with a delay shorter than one utility period.

The simulation result in Fig. 6(d) describing the response of the DSRF-PLL in the detection of the amplitude of the positive sequence voltage component is very close to that one shown in Fig. 4 (k=0,707), which was obtained analytically. The slight differences between both figures are due to $\theta' \neq \omega t$ during the stabilization period of the PLL.

From the simulation results shown in this section it is possible to state that the DSRF-PLL eliminates completely the well kwon problems of the SRF-PLL when the utility voltage is unbalanced [9] and achieves higher performance than other systems designed with the same purpose [7].

V. EXPERIMENTAL RESULTS

In order to ratify the simulation results, the scenario previously simulated has been physically implemented using an ELGAR SM5250A programmable AC source and a dSpace DS1103 DSP board as a control system.

For the first experiment, the values for the different parameters are maintained equal to those ones used previously to obtain the waveforms shown in Fig. 6. For the implementation of the DSRF-PLL algorithm on the DSP, the sampling time was defined equal to 50μS. In such conditions, the characteristic waveforms from the experiment are shown in Fig. 7. Note how these waveforms are almost equal to the waveforms simulated previously, which should not be surprising since the sampling period is much smaller than the time constant of the system. In Fig. 7, a new signal, $\bar{v}_{Sq^{+1}}$ is added.

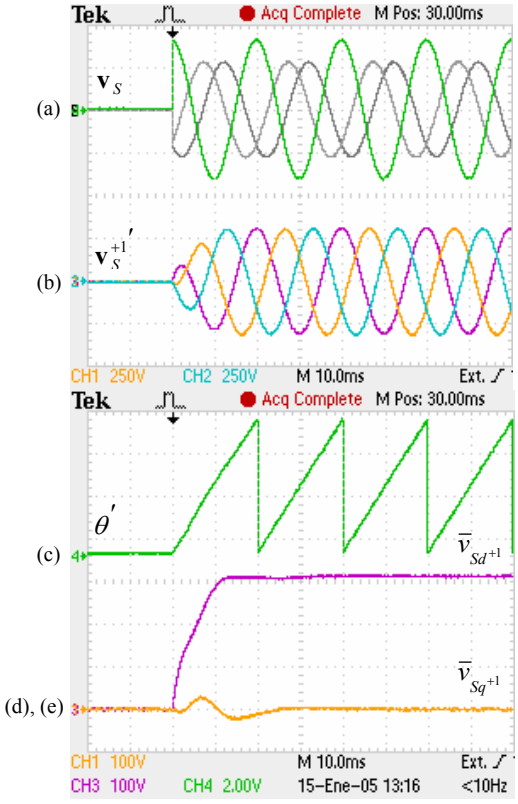

Fig. 7: Characteristic waveforms at the start up of the SDRF-PLL.

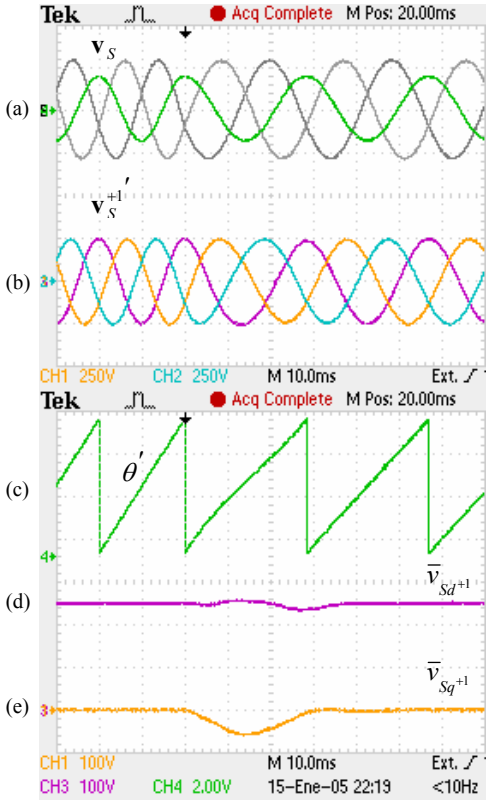

Fig. 8: Characteristic waveforms when the utility frequency varies.

Logically, after the stabilization period, which is approximately equal to a grid period, the signal $\bar{v}_{Sq^{+1}}$ is equal to zero.

One of the most important features of a PLL-based structure respect to other techniques is its capability of adaptation to changes in the utility frequency. For testing this characteristic in the DSRF-PLL, most of its parameters were held equal to those ones used in the previous experiment, and only the value for k was changed to $k = 1/2$ in order to increase the damping in the system response. Fig. 8 depicts the behavior of the proposed DSRF-PLL when the utility frequency suddenly changes from 50Hz to 35Hz. This frequency decreasing (30%) is twice higher than the maximum variation admissible in the standard EN-50160 for isolated networks. Fig. 8 shows how the DSRF-PLL offers good results even if, under unbalanced conditions, a non-negligible variation appears in the utility frequency. This is a really interesting characteristic for the use of the DSRF-PLL in the control of power electronics systems applied to wind generators [2], mainly when these generators are working in island mode.

In previous explanations in this paper, only positive and negative sequence components at fundamental frequency were considered, without high-order voltage harmonics. It is well known that bandwidth reduction in the conventional SRF-PLL minimizes the influence of high-order harmonics over the system output. However, it also reduces the system dynamics.

To evaluate how the bandwidth reduction is an acceptable solution for the DSRF-PLL when the utility voltage is strongly distorted, an unbalanced fifth harmonic component is added to the utility voltage. Now, the utility voltage is characterized by $V_S^{+1} = 80V$, $V_S^{-1} = 20V$, $V_S^{+5} = 10V$, and $V_S^{-5} = 10V$. The waveforms shown in Fig. 9 are obtained using the same parameters for the DSRF-PLL as in the previous case. In Fig. 9, it is possible to appreciate how slight oscillations appear in θ', $\bar{v}_{Sd^{+1}}$, and $\bar{v}_{Sq^{+1}}$ signals when the utility voltage is distorted, which gives rise to a certain distortion in the reconstruction of the positive sequence component at fundamental frequency (see Fig. 9(b)). Although these results could not seem good, it is worth noting that the actual utility voltage is usually less distorted than that one considered in this experiment. Moreover, the distortion in the detected waveforms could have been attenuated by means of bandwidth reduction in the PLL, or increasing the order of the LPF; however, these measures would slightly slow down the dynamic response of the system. For those applications in which a really fast and precise response is required, a new detector based on multiple synchronous reference frames (MSRF-PLL) can be used. This detector will be presented in future papers and uses multiple DCs for insolating all the voltage components.

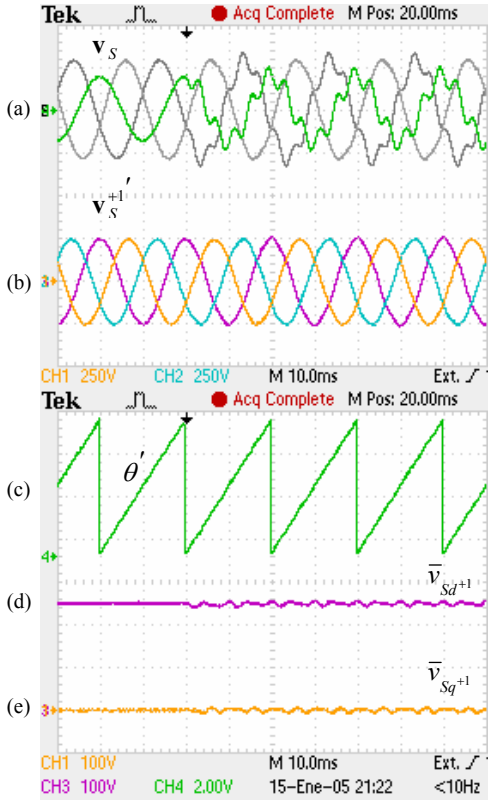

Fig. 9: Characteristic waveforms when the utility voltage is distorted.

VI. CONCLUSION

The study and results presented in this paper evidence that the DSRF-PLL is a suitable solution to one of the main problems that appears when using conventional PLL systems, namely detection of positive sequence fundamental component of the utility voltage in a robust way, even under unbalanced and distorted grid conditions.

This paper offers an analytical sound approach for the utility voltage characterization based on the use of two synchronous reference frames (DSRF-PLL). Using the DSRF together with the DN permits to insolate the positive and negative voltage components and free-error detection is achieved in a very fast way. Hypotheses and assumptions adopted in the theoretical study of the DSRF-PLL are ratified by simulation and experimental results. The proposed approach can be extended toward more generic scenarios, where not only two, but more voltage components should be isolated. This new detector, based on multiple synchronous reference frames (MSRF-PLL), will be reported in a future paper.

ACKNOWLEDGMENT

This work was supported by the Departament d'Universitats, Recerca i Societat de la Informació of the Generalitat de Catalunya, under grants 2004BE00060 and 2004BE00150, and by the Ministerio de Ciencia y Tecnologia of Spain under Project ENE2004-07881-C03-02.

This work made use of Engineering Research Center Shared Facilities supported by the National Science Foundation under NSF Award Number EEC-9731677 and the CPES Industry Partnership Program. Any opinions, findings and conclusions or recommendations expressed in this material are those of the authors and do not necessarily reflect those of the National Science Foundation.

REFERENCES

[1] M. Cichowlas, M. Malinowski, D.L. Sobczuk, M.P. Kazmierkowski, P. Rodríguez, and J. Pou, "Active filtering function of three-phase PWM boost rectifier under different line voltage conditions," *IEEE Trans. Ind. Electron.*, vol. 52, pp. 410-419, Apr. 2005.

[2] R. Teodorescu and F. Blaabjerg, "Flexible control of small wind turbines with grid failure detection operating in stand-alone and grid-connected mode," *IEEE Trans. Power Electron.*, vol. 19, pp. 1323-1332, Sep. 2004.

[3] A. Ghosh and A. Joshi, "A new algorithm for the generation of reference voltages of a DVR using the method of instantaneous symmetrical components," *IEEE Power Eng. Review*, vol. 22, 2002, pp. 63-65.

[4] H. Song, H. Park, and K. Nam, "An instantaneous phase angle detection algorithm under unbalanced line voltage condition," in *Proc. IEEE Power Electron. Spec. Conf.*, vol. 1, 1999, pp. 533-537.

[5] L.N. Arruda, S.M. Silva, B.J.C. Filho, "PLL structures for utility connected systems," in *Proc. IEEE Ind. Applicat. Conf.*, vol. 4, 2001, pp. 2655-2660.

[6] P. Rodríguez, L. Sainz, and J. Bergas, "Synchronous double reference frame PLL applied to a unified power quality conditioner," in *Proc. IEEE Int. Conf. Harm. and Power Quality*, vol. 2, 2002, pp. 614-619.

[7] M. Karimi-Ghartemani and M.R. Iravani, "A method for synchronization of power electronic converters in polluted and variable-frequency environments, " *IEEE Trans. Power Systems*, vol. 19, 2004, pp. 1263-1270.

[8] V. Kaura and V. Blasco, "Operation of a phase locked loop system under distorted utility conditions," *IEEE Trans. Ind. Applicat.*, vol. 33, 1997, pp. 58-63.

[9] S. Chung, "A phase tracking system for three phase utility interface inverters," *IEEE Trans. Power Electron.*, vol. 15, 2000, pp. 431-438.

[10] S. Lee, J. Kang, and S. Sul, "A new phase detecting method for power conversion systems considering distorted conditions in power systems," in *Proc. IEEE Ind. Applicat. Conf.*, vol. 4, 1999, pp. 2167-2172.